High Pressure and High Temperature Study on Lithium carbide (Li_2C_2) and Calcium carbide (CaC_2): An attempt to make a novel polyanionic form of Carbon

by

Sumit Konar

A Thesis Presented in Partial Fulfillment
Of the Requirements for the Degree
Master of Science

Approved August 2012 by the
Graduate Supervisory Committee:

Ulrich Häussermann, Co-Chair
Dong Seo, Co-Chair
Timothy Steimle
George Wolf

ARIZONA STATE UNIVERSITY

December 2012

ABSTRACT

Carbon lacks an extended polyanionic chemistry which appears restricted to carbides with C^{4-}, C_2^{2-}, and C_3^{4-} moieties. The most common dimeric anion of carbon atoms is C_2^{2-} with a triple bond between the two carbon atoms. Compounds containing the dicarbide anion can be regarded as salts of acetylene C_2H_2 (ethyne) and hence are also called acetylides or ethynides. Inspired by the fact that molecular acetylene undergoes pressure induced polymerization to polyacetylene above 3.5 GPa, it is of particular interest to study the effect of pressure on the crystal structures of acetylides as well. In this work, pressure induced polymerization was attempted with two simple metal acetylides, Li_2C_2 and CaC_2. Li_2C_2 and CaC_2 have been synthesized by a direct reaction of the elements at 800ºC and 1200ºC, respectively. Initial high pressure investigations were performed inside Diamond anvil cell (DAC) at room temperature and *in situ* Raman spectroscopic measurement were carried out up to 30 GPa. Near 15 GPa, Li_2C_2 undergoes a transition into a high pressure acetylide phase and around 25 GPa this phase turns amorphous. CaC_2 is polymorphic at ambient pressure. Monoclinic CaC_2-II does not show stability at pressures above 1 GPa. Tetragonal CaC_2-I is stable up to at least 12 GPa above which possibly a pressure-induced distortion occurs. At around 18 GPa, CaC_2 turns amorphous. In a subsequent series of experiments both Li_2C_2 and CaC_2 were compressed to 10 GPa in a multi anvil (MA) device and heated to temperatures between 300 and 1100°C for Li_2C_2, and 300°C to 900°C for CaC_2. The recovered products were analyzed by PXRD and Raman spectroscopy. It has been observed that reactions at temperature

higher than 900°C were very difficult to control and hitherto only short reaction times could be applied. For Li_2C_2, a new phase, free of starting material was found at 1100°C. Both the PXRD patterns and Raman spectra of products at 1100°C could not be matched to known forms of carbon or carbides. For CaC_2 new reflections in PXRD were visible at 900°C with the starting material phase.

ACKNOWLEDGMENTS

I am extremely fortunate to have Dr. Ulrich Häussermann as my supervisor. I would like to thank him sincerely for his instruction and guidance for every minute detail regarding experiments, analyzing data, searching literature and my writing dissertation. His knowledge, way of finding truth from a failed experiment and modifying the procedure in the next step really helped me to think critically and without any bias. He is the man who led me to the leeway of solid state chemistry.

I would like to take this opportunity to acknowledge the great help provided by my committee members, Dr. Don Seo, Dr. Timothy Steimle and Dr. George Wolf through helpful discussions and moral support during my stay at ASU. I also would like to thank Dr. Kurt Leinenweber for sharing his tremendous experience in multi-anvils. I spend most of the time in the high pressure lab after the group moved to Stockholm. I also want to thank Dr. Tom Groy for his expertise in the crystallography and Dr. Emmanuel Soignard for guiding me to learn Raman spectroscopy. Special thanks to Wilhelm Klein in Munich for performing high temperature XRD of one of my sample.

I would like to thank all of my past and present group members. Special thanks to Dr. Yang Wu for constantly encouraging me to read articles and to Dr. Johanna Nylen for helping me with diamond anvil cell experiments. Kati, Verina and Kristina are omnipresent whenever needed and retain a cheerful atmosphere around the lab. Help at my department is not limited to my own group; Craig, Amber, Alex, Dinesh, Kiwan, and Soham helped me whenever I asked. Thank

you all. I also want to thank my friends in Arizona State University. Special thanks to Sriloy, Aritra, Subhadip, Suratna, Arnab, and Souvik.

At the end, appreciation from the core of my heart goes to my dear family members, my mother, brother, sister and last but not the least my fiancée Utsa, for being at my side all the time.

TABLE OF CONTENTS

Page

LIST OF TABLES

LIST OF FIGURES

Figure Page

Figure Page

CHAPTER 1

INTRODUCTION

When applying external pressure, acetylene undergoes polymerization to polyacetylene. Evidence of pressure-induced solid state polymerization has been reported in acetylene from vibrational spectroscopy inside Diamond Anvil Cell (DAC). Aoki *et al.* studied the mechanism and kinetics of pressure induced polymerization by Raman spectroscopy and reported the incidence of polymerization reaction in the orthorhombic phase at room temperature and pressure above 3.5 GPa.[1] The colorless starting material turned deep red upon polymerization. The reaction was later investigated by infrared spectroscopy by Sakashita *et al.*[2] They found that both conjugated and saturated polymers were formed simultaneously when the reaction was initiated at 4.2 GPa. In 2000, Chad *et al.* reported that at low temperature (77 K) polymerization of acetylene began at higher pressure around 12.5 GPa and the reaction was completed during release of pressure at 2.5 GPa.[3] Ceppatelli *et al.* studied the pressure and laser induced polymerization of solid acetylene by FTIR spectroscopy.[4] They concluded that pressure prompts an orderly growth of trans-polyenic species; while irradiation yields the opening of the double bonds and branching of the chains take place consequently. In the molecular dynamics simulation study by Bernasconi *et al.*, *cis*- and *trans*- polyenic chains were observed with substantial cross linking between the chains.[5] The reaction was found to occur only at 400K and pressure of 25 GPa, a threshold pressure much higher than that observed experimentally.

Several carbides correspond to salts of the acetylide anion C_2^{2-} e.g., lithium carbide (Li_2C_2), sodium carbide (Na_2C_2), calcium carbide (CaC_2), magnesium carbide (MgC_2) and lanthanum carbide (LaC_2). C_2^{2-} is isoelectronic to C_2H_2. Applying pressure to acetylide-like carbides may provide the opportunity to achieve chain like, ribbon like and layer like nominally charged carbon structures stabilized by electrostatic interactions from the surrounding cations. In contrast with the various forms that exhibit two and three dimensional backbones of carbon atoms, ligand free chain-like structures have not yet been realized. This would add a new aspect to carbon chemistry, and materials containing or consisting of polymeric carbon anions can be expected to exhibit interesting optical, mechanical and electron transport properties. Especially superconductivity of relevant material is interesting and fueled by the recent discovery of several superconducting carbon based materials, which include graphite-intercalated-compounds (GIC)[6,7], e.g. CaC_6, KC_8 and alkali metal fullerides.

In this work, the pressure induced polymerization of anions (C_2^{2-}) present in acetylides like Li_2C_2 and CaC_2 has been attempted. There are only a few reports on high pressure studies of acetylides. In metal acetylides, the bonds between the carbon atoms in the dumbbells are “covalent” in nature whereas the interaction between metal and C_2^{2-} is “ionic”, so they are of mixed covalent-ionic bonding environment. Kulkarni *et al.* computationally explored the enthalpy landscape of CaC_2 on the *ab initio* level by employing a simulated annealing algorithm as a global exploration method.[9] It was found that at pressures above 30 GPa the six-

fold coordination of C_2^{2-} units by Ca^{2+} ions (similar to NaCl structure), which is characteristic of ambient pressure structures, becomes unstable with respect to a denser packing with 8-fold coordination (similar to CsCl structure). The postulated denser packed dumbbell structure was later experimentally verified for a high pressure polymorph of BaC_2.[10] BaC_2 transforms from the tetragonal ground state structure, at around 4 GPa, to an eight-coordinated rhombohedral modification (space group *R*3*m*), (distorted CsCl-type structure). A second high pressure transition occurs at 33 GPa to a more or less amorphous polymorph. Pressure induced amorphization, at 13 GPa, was also observed for LaC_2 which has the same ground state structure as BaC_2[11]. Finally, and most relevant to this study, a computational study[12] by Chen *et al.* suggested the accessibility of polymeric carbon chains from the pressure treatment of Li_2C_2 and which, according to this study, at around 5 GPa is expected to transform into the CrB structure with zigzag chains of carbon atoms. This transformation is driven by a large volume reduction of about 25%.

Lithium carbide (Li_2C_2) and calcium carbide (CaC_2) were chosen to study the polymerization of acetylide under high pressure. An *in situ* raman spectroscopic study inside diamond anvil cell was performed with both Li_2C_2 and CaC_2 at room temperature up to 30 GPa pressure. A wide range of high pressure syntheses with both Li_2C_2 and CaC_2 at different pressure and temperature conditions was done in multi anvil apparatus. The products obtained were characterized with powder XRD and Raman spectroscopy.

CHAPTER 2

EXPERIMENTAL METHODS

2.1 Synthesis of acetylides:

All steps of sample preparation were performed in an Argon-filled glove box (H_2O concentration < 0.3 ppm and O_2 concentrations <0.1 ppm). Starting materials were rods (Φ=12.7 mm, l~165 mm) of Li (99.9%), dendritic calcium (99.8 %) and graphite powder (99.9%)

Li_2C_2:

A nearly quantitative synthesis of microcrystalline Li_2C_2 was reported by Juza, Wehle, and Schuster by a reaction between lithium vapor and amorphous coal or graphite in a steel container at temperatures between 800ºC and 900°C.[13] The synthesis has been modified by taking stoichiometric amounts of lithium metal and graphite powder in a tantalum (Ta) ampoule. Li metal is sensitive to moisture. The surface of lithium metal was scratched with a razor blade prior to the synthesis to remove impurities. Lithium metal pieces were cut with pliers and sandwiched between top and bottom layers of graphite powder in a Ta ampoule. Both sides of the Ta ampoule were arc-welded inside glove box. The ampoule was placed inside quartz tube, and kept in RF furnace at 800ºC for 1h under vacuum. The samples were allowed to cool by turning off the furnace and then returned back to glove box, where it was opened and ground to powder in a

mortar with a pestle. The product was white or grayish in color. The phase purity of the product was checked with powder X-ray diffraction.

CaC_2:

Synthesis of pure CaC_2 was reported by Ruschewitz *et al* by the reaction between elemental calcium and graphite in a graphite cylinder at about 800ºC inside a horizontal tube furnace for about sixteen hours.[14] The synthesis has been modified by reducing the reaction time to three hours and raising the temperature to 1200 ºC. For the synthesis of 200 mg sample, calcium (120.48 mg, 3.01 mmol) and graphite (79.52 mg, 6.62 mmol) were mixed in a molar ratio of 1:2.2 inside the glove box and pressed to a pellet of Φ = 8 mm. The pellet was taken in a Ta ampoule. Both sides of the Ta ampoule were arc welded inside the glove box and was put inside quartz tube outside the glove box. The quartz tube was kept at 1200ºC for 3 hours in RF furnace. The sample was allowed to cool to room temperature and transferred to the glove box where further handling was carried out. The phase purity of the product was checked with x-ray Powder Diffraction.

2.2 High Pressure Experiments:

High pressure experiments are usually carried out either in (1) Diamond Anvil Cell (DAC),or in (2) Multi Anvil (MA) press.[15] In DAC studies pressures from 0.1 to several hundred GPa (0.1 GPa = 10^8 Pa = 1 kbar ≈ 1000 atm) can be achieved within tiny samples (0.1 mm^3 or even smaller) held between two opposed diamond anvils. Due to the transparency of diamond anvils for X-rays, infrared and visible light, many properties of the compressed sample can be measured *in situ* by spectroscopy and diffraction. The small sample size however limits the DAC as an observatory tool. To obtain the large sample yields, for *ex situ* characterization of structural, chemical, and physical properties of reaction products multi anvil apparatus should be used. This anvil device is driven by a large hydraulic press and pressure is applied on the sample from several directions simultaneously. The pressure range that can be reached in a MA device is obviously lower than in the DAC (typically up to 25 GPa), but sample temperatures and the synthesis environment are much better controlled in MA. In DAC, simultaneous heating can be achieved either internally through an infrared laser or externally through electrical (resistive) heating. In multi-anvil devices, high temperatures can be attained by inserting a resistive furnace (usually made of graphite or $LaCrO_3$) into the pressure transmitting medium around the sample. In multi-anvil press and in externally heated diamond cells, temperature is most conveniently measured by thermocouples whereas in laser-heated diamond cells,

temperature can be determined by measuring the spectral distribution of the emitted blackbody radiation.

Diamond Anvil Cell Experiments:

DAC experiments were carried out in a Diacell (Merrill-Bassett type) instrument. The diamonds were always mounted on some support plate ("seat") made out of a hard material, usually tungsten carbide. This design allowed the seats to be tilted and moved horizontally, in order to make sure that the culets of the diamonds were exactly parallel and the culets were matching. Load was applied by means of two bolts, one of which had a left-handed thread. This arrangement allowed a symmetrical load to be applied to the anvils, while no net twisting was put on the device. No pressure transmitting medium was used since Li_2C_2 and CaC_2 are extremely sensitive to moisture and readily hydrolyzes with common pressure-transmitting media, such as methanol/ethanol or silicone oil. Stainless steel gaskets with an initial thickness of 250 μm were indented to 60 μm. The sample compartment corresponded to a 150 μm diameter central hole which was pressurized using 300 μm culet diamonds. For monitoring the pressure the ruby fluorescence line shift was employed.[16] Accordingly, a small chip of ruby crystal was placed along with the sample in the gasket aperture.

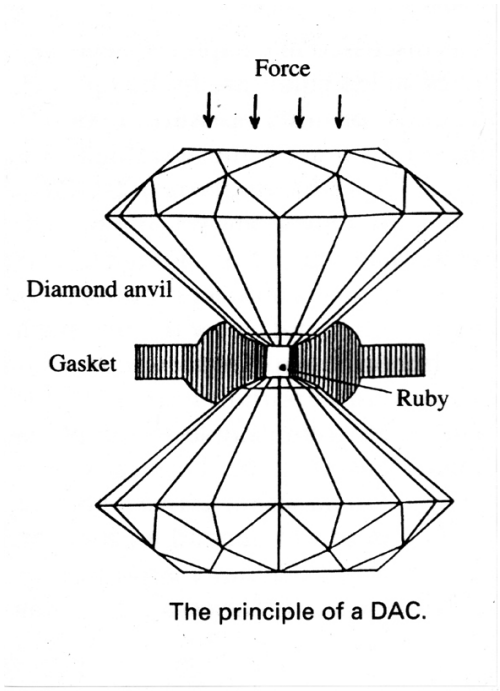

a) b)

Figure 1. Diamond anvil cell (DAC) (a) Schematic diagram and (b) real apparatus

Multi-Anvil (MA) Experiments:

High pressure experiments were carried out in a 6–8 Walker-type MA high pressure module. The six steel wedges (outer anvil) created a cubic cavity for the inner anvils and were placed in a confinement ring. The module was compressed in a hydraulic press (maximum uniaxial load of 1000t). The inner anvil was made of eight 25 mm edge length tungsten carbide (WC) cubes with truncated corners. The corner truncations of the WC cubes created an octahedral cavity at the centre, in which a ceramic pressure-transmitting medium was placed. Typically a castable ceramics with a composition of 55 weight percentage MgO and 45 weight percentage spinel and a porosity of about 20 volume percentage was used.[17] By varying the Truncation Edge Length (TEL) and the Octahedral Edge Length (OEL) of the pressure medium different pressure ranges could be attained. For most of our MA runs a 18/12 assembly was used (OEL= 18 mm, TEL= 12 mm). To support the truncations and seal in the high-pressure region, gaskets, normally of pyrophyllite, were placed between the anvils.

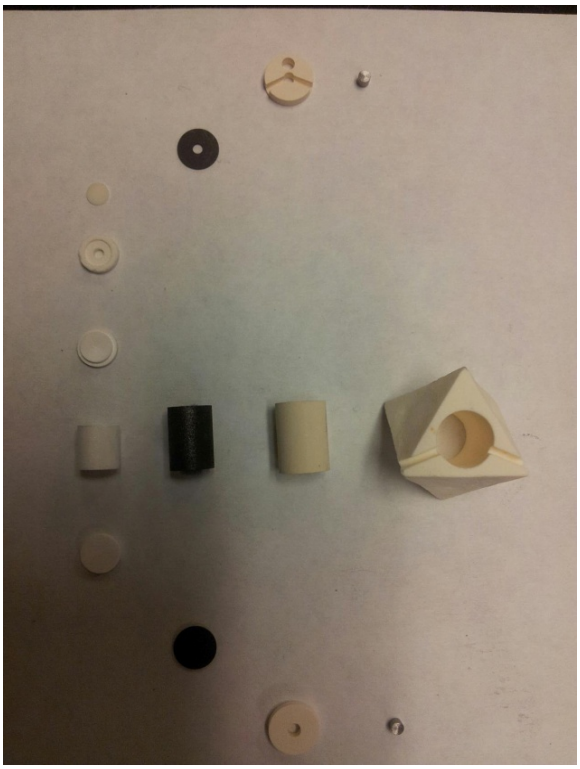

a)

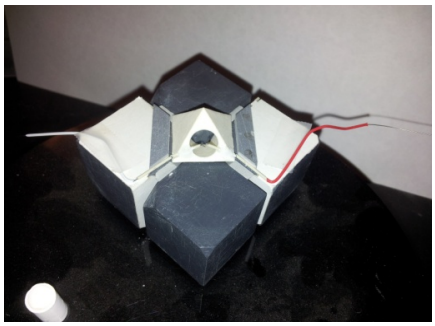

b)

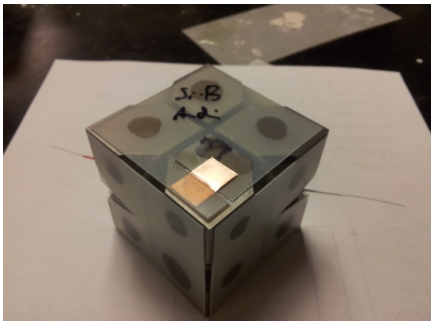

c)

Figure 2. Assembly of multi anvil apparatus, (a) parts (b) octahedron is nested in the cavity of cubes with truncated edges, (c) closed cubes with octahedron inside, ready to go inside multi anvil

Samples were loaded either inside hexagonal BN capsule (h-BN) or salt (NaCl) capsule inside Ar filled glove box (oxygen concentration is less than 0.1 ppm). The inner diameter (ID) and outer diameter (OD) of both type of capsule

were 4 mm and 6.1 mm respectively. Length of the h-BN and salt capsules were 7.3 mm and 8 mm respectively. The shorter length of BN capsule was compromised with MgO disk. The capsule was taken out from the glove box and positioned inside a graphite furnace. This arrangement was then placed together with a zirconia thermal insulating sleeve inside a magnesia octahedron. After reaching the target pressure the samples were heated slowly to temperatures. The temperature was measured close to the sample using a thermocouple type C (W5%Re–W26%Re wire) in an Al_2O_3 sleeve. Afterward, the pressure was released over a period of several hours and the samples were recovered in the glove box.

2.3 Differential Thermal Analysis:

Differential Thermal Analysis (DTA) experiments were carried out in a Shimadzu DTA-50 instrument. Powder Li_2C_2 sample was sealed in a stainless steel capsule inside the glove box. Temperature was increased at a rate of 10ºC per minute till 1100ºC and cooling process was done at a rate of 10ºC per minute. A constant Argon flow during the experiment was maintained.

2.4 High temperature XRD measurement:

The measurement was performed on a Stadi P diffractometer from Stoe with Cu tube and myths detector. The temperature adjustment was performed using a

Stoe Kapillarofens. The furnace consisted of a graphite rod, which was enclosed by a water-cooled metal cylinder. The interior of the furnace during the heating phases were kept under nitrogen atmosphere to prevent oxidation of the graphite rod. Temperature was measured with a Pt / Rh thermocouple. In an about 0.6mm thick longitudinal hole of the graphite rod, maximum 0.5mm thick capillaries were introduced. A wide transverse bore allowed the passage of the X-rays.

2.5. **Powder X-ray Diffraction**:

The highly moisture sensitive products were analyzed by powder X-ray diffraction. Samples were ground and loaded into 0.3 mm glass capillaries inside the glove box. Measurements were performed on a Bruker D8 Advanced diffractometer (Göbel mirror, Cu Kα radiation) for a 2θ range from 10º to 90º with an increment step of 0.008°.

2.6 Raman Spectroscopy:

The Raman data were collected using a custom built Raman spectrometer in 180º geometry. The sample was excited using a 532 nm laser. The laser power was adjusted using neutral density (ND) filters. The laser was focused using a 50X super long working distance objective (Mitutoyo). The numerical aperture of

the objective was 0.42. The signal was separated from the laser excitation using two filters; first a Kaiser laser band pass filter was used and it was followed by a Semrock edge filter. A liquid nitrogen cooled CCD detector was used. After X-ray diffraction measurement, the same capillary was mounted on a clean glass slide. Laser power of 0.65 mW was used. Increase of laser power caused burning of the sample/glass capillaries. The image was observed using PixeLink software.

CHAPTER 3

RESULTS AND DISCUSSION

3.1. Ambient pressure investigation of CaC_2 and Li_2C_2

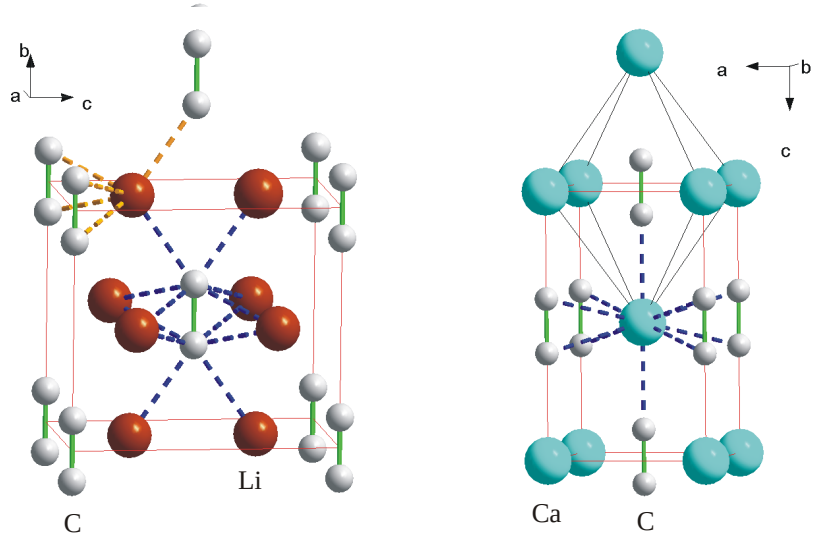

(a) (b)

Figure 3. Crystal structure of (a) Li_2C_2 [Immm (No. 71), Z = 2] and (b) CaC_2 -I [I4/mmm, Z=2]

Figure 3 has been drawn by collecting the crystallographic information from literature (Ruschewith *et al.*) and with the help of Diamond software.

3.1.1 CaC_2

In literature, CaC_2 is reported to exist in four modifications. In 2001, Ruschewitz *et al.* reported about the phase transition of CaC_2 in detail and discussed all of these four modifications with reference to all the previous work

on CaC_2.[14] At room temperature CaC_2 exists as a body centered tetragonal modification CaC_2-I (I4/mmm, Z=2) where C_2^{2-} dumbbells align along the tetragonal axis. In CaC_2-I, each Ca atom is coordinated by four C_2^{2-} dumbbells in a side-on fashion and two C_2 dumbbells in an end-on organization that leads to a overall coordination number 8+2. This tetragonal form converts to a low temperature monoclinic form CaC_2-II (C2/c, Z=4.) This form crystallizes in the ThC_2 structure type. There is also a meta stable modification CaC_2-III (C2/m, Z=4). A cubic high temperature modification of CaC_2 -IV (Fm-3 m, Z=4) is found at 490°C. The crystal structure of CaC_2-I is depicted in figure 3(b).

Crystalline powders of CaC_2 without any impurities were obtained by the reaction between graphite and elemental calcium. The colors of the resulting samples were light to dark gray. The color obtained depends upon the reaction condition. The obtained samples were characterized with X-ray powder diffraction and Raman spectroscopy. Powder XRD revealed the presence of all the three modifications reported in literature. Powder X-ray diffraction patterns were plotted and compared with literature. The presence of CaC_2 -III appeared to be really small, and sometimes it was not formed at all. It was found that CaC_2 -I and CaC_2 -II were the major phases in the sample. Long synthesis time and small scale sample preparation favored the tetragonal phase CaC_2-I over the monoclinic phase CaC_2-II.

From diffraction patterns shown in figure 4 it can be understood that small scale sample preparation favored CaC_2-I phase, if the reaction temperature and reaction time were kept constant. Diffraction patterns in figure 5 show that longer

reaction time favored CaC_2-I phase over the CaC_2-II, if the reaction temperature and sample amount were kept constant. In figure 5 some additional reflections are visible in 1.5 hour experiment, which are shown as red and blue arrows. Red arrows correspond to TaC (F m -3 m) phase whereas blue arrows correspond to Ta_2C (P 63/m m c) phase. Probably during reaction Ta material from the ampoule reacted with graphite and formed tantalum carbides. Scratching sample from Ta

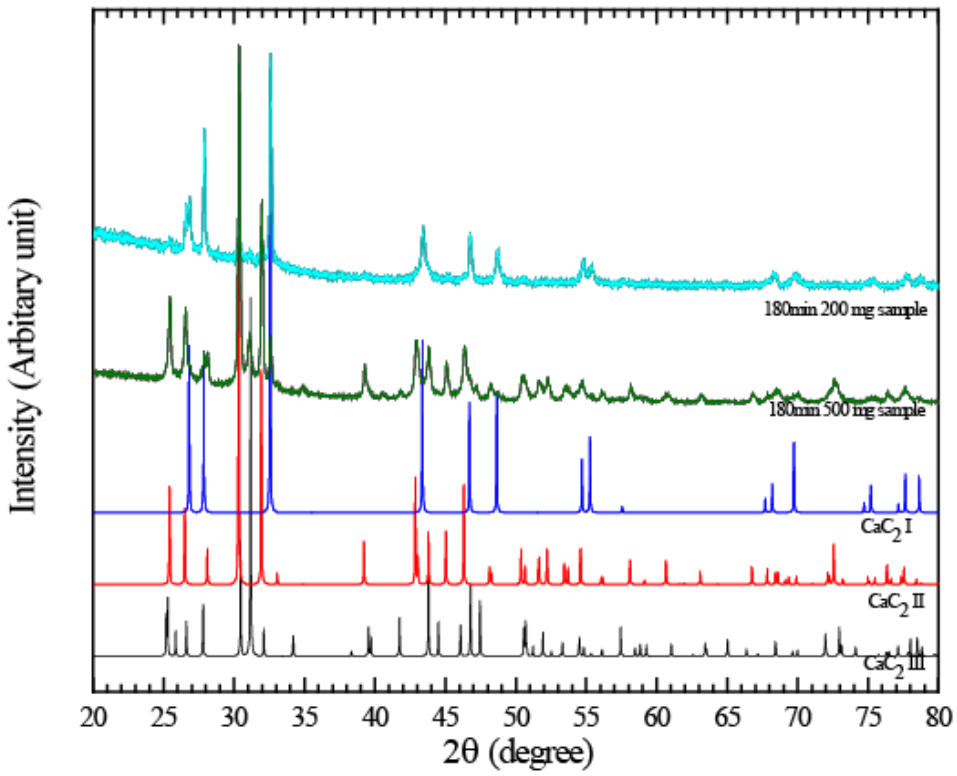

Figure 4. Powder XRD of CaC_2 starting material, longer reaction time favors CaC_2-I phase over CaC_2-II phase

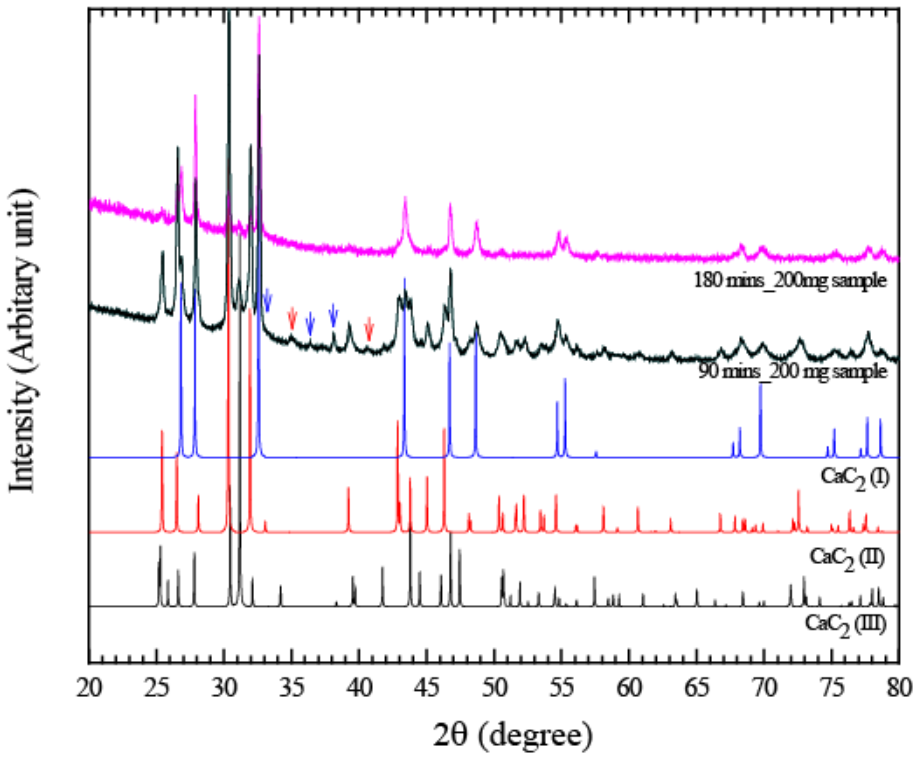

Figure 5. Powder XRD of CaC_2 starting material, smaller sample amount favors CaC_2-I phase over CaC_2-II phase. Red arrows correspond to TaC (F m -3 m) phase where blue arrows correspond to Ta_2C (P 63/m m c) phase

ampoule caused these tantalum carbides impurities and hence was avoided for all other syntheses of calcium carbide.

The Raman spectra of CaC_2 at ambient pressure and room temperature are shown in figure 6. The wavenumbers of Raman active modes for CaC_2-I and II, are compiled in Table-I with the help of literature.[18] The spectra of CaC_2 is divided into two regions: C-C stretches have large intensities and occur at higher wavenumbers (between 1800 and 1900 cm^{-1}) whereas libration modes of C_2

dumbbells and translation modes, which comprise mostly of displacements of the metal ions, have low intensities and is obeserved at wavenumbers below 500 cm^{-1}. The first-order Raman spectrum of tetragonal CaC_2-I constitutes of the C-C stretching mode (A_{1g}) and the double degenerate libration of C_2 dumbbells (E_g). These bands are observed at 1864 and 311 cm^{-1}, respectively. Monoclinic CaC_2-II has two formula units in the primitive unit cell and eight Raman modes are expected.

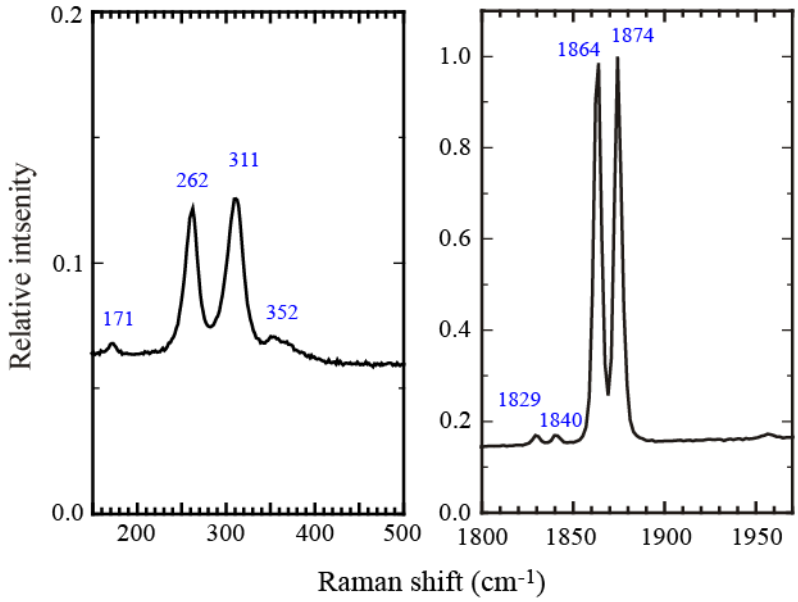

Figure 6. Raman spectrum of CaC_2 at ambient pressure and room temperature, libration modes are much less intense

These are two C-C stretches, four librations and two translation modes. In the spectrum of CaC_2 only one stretch is observed at 1874 cm^{-1}. Three libration

modes occur at 352, 262, and 171 cm^{-1} respectively. The fourth libration mode most likely overlaps with the CaC_2-I single libration mode. The contribution from ^{13}C and ^{12}C to the C-C stretch vibration of CaC_2-I and II is separated by about 35 cm^{-1}.

Table-I Compilation of Raman active stretching and libration modes for CaC_2

CaC_2-I (D_{4h})		CaC_2-II (C_{2h})	
Experimental (cm^{-1})	Raman active mode	Experimental (cm^{-1})	Raman active mode
1864	A_{1g}	-	B_g
		1874	A_g
311	E_g	352	lib B_g
		~311	lib B_g
		262	lib A_g
		171	lib B_g
		-	trans A_g
		-	trans B_g

3.1.2 Li_2C_2:

Li_2C_2 occurs in two forms. At room temperature the structure is reported to be orthorhombic (space group Immm (No. 71).[19] Li_2C_2 crystallizes isotypic to Rb_2O_2 and Cs_2O_2. The crystal structure of Li_2C_2 is depicted in figure 3(a). The C_2^{2-} dumbbells are aligned parallel to the *b* axis of the orthorhombic unit cell. Each C_2^{2-} dumbbell is coordinated by eight Li cations, four in a side-on and four in an end-on fashion. Each Li cation is coordinated side-on and end-on to two C_2^{2-} dumbbells. so that overall obtained co-ordination number is 6. There is a phase transition to high temperature cubic anti-CaF_2 structure at 420°C.

Crystalline powders of Li_2C_2, without any impurities, were obtained by the reaction between elemental lithium and graphite. The samples were grayish white, bluish white to pure white. The color depended on the stoichiometry of lithium used. A perfect 1:1 stoichiometry of lithium and graphite led to the formation of complete white sample. A tiny amount of excess graphite formed a sample gray in color whereas the crystallization of Li_2C_2 from a little excess of metallic lithium produced bluish white sample, which is also reported in literature.[19] The resulting samples were characterized with X-ray powder diffraction and Raman spectroscopy. Powder XRD revealed the presence of low temperature orthorhombic modification reported in literature. Powder X-ray diffraction pattern is plotted and compared with literature.

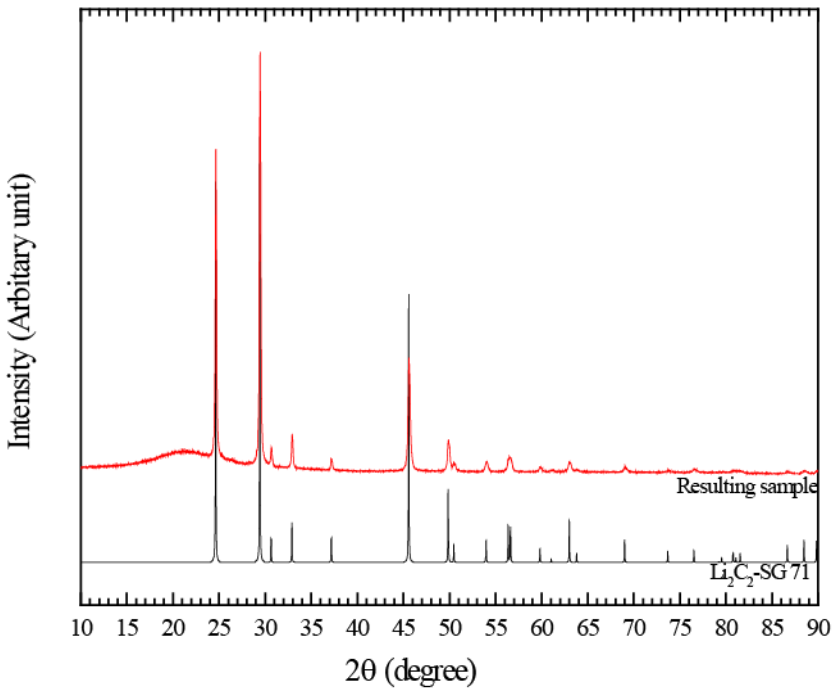

Figure 7. X-ray powder diffraction pattern for Li_2C_2 recorded at room temperature (Immm, No. 71, Z = 2)

.

The Raman spectra of Li_2C_2 at ambient pressure and room temperature are shown in figure 8. The wavenumbers of Raman active modes for Li_2C_2 are compiled in Table-II with the help of literature.[18] The spectra of Li_2C_2 are divided into two regions, like CaC_2. Orthorhombic Li_2C_2 contains four atoms in the primitive unit cell, hence nine optic modes are expected. Out of these nine optic modes, six are Raman active: the C-C stretch, two librations and three translation modes. The former modes are clearly visible in the spectrum of figure 8 and appear at 1872, 318 and 284 cm^{-1}, respectively. The stretching mode contribution from ^{13}C and

^{12}C is at 1838 cm^{-1}. The weak feature, at around 390 cm^{-1}, may be assigned to the B_{3g} translation (Table-II).

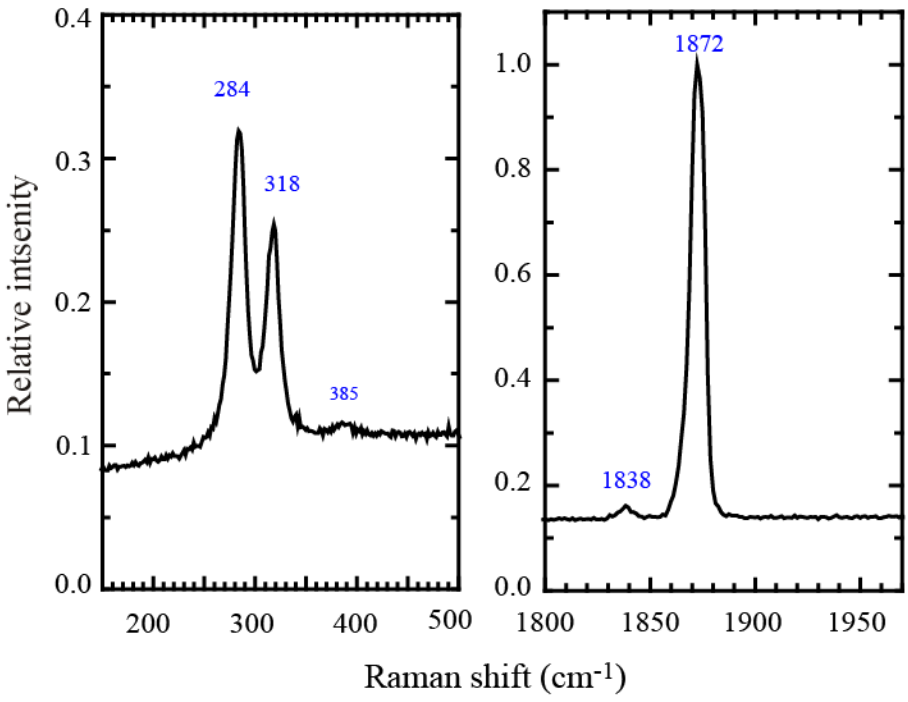

Figure 8. Raman spectrum of Li_2C_2 at ambient pressure and room temperature, libration modes are much less intense

Table-II Compilation of Raman active stretching and libration modes for Li_2C_2

Li_2C_2 (D_{2h})	
Experimental (cm^{-1})	Raman active mode
1872	A_g
-	trans A_g
385	trans B_{3g}
318	lib B_{1g}
-	trans B_{2g}
284	lib B_{3g}

3.1.2a Results of DTA experiments with lithium carbide:

A phase transition of Li_2C_2 from orthorhombic to a cubic anti-CaF_2 structure with disordered C_2 dumbbells was found in literature at a temperature of about 420ºC. DTA measurement with Li_2C_2 showed a phase transition around 426ºC, which supports literature value. The DTA measurement indicates another phase transition around 763ºC which needs more investigation.

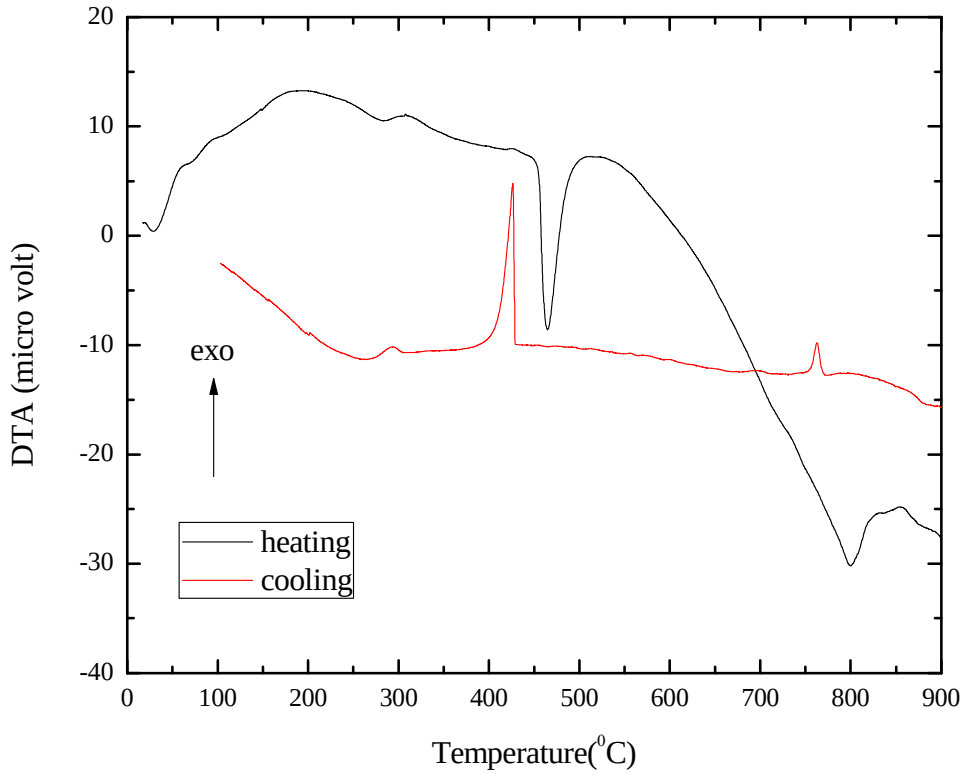

Figure 9. DTA experimental results for lithium carbide (Li_2C_2)

3.1.2b High temperature XRD experiment with Li_2C_2:

The first phase transition at about 420ºC was investigated, see figure 10 (the plot of the temperature program starts at the bottom). The cubic phase appeared at 460ºC, the conversion was complete at 475ºC. On cooling, the orthorhombic modification appeared again only at 435ºC, the cubic could be seen again at 405ºC, though weak.

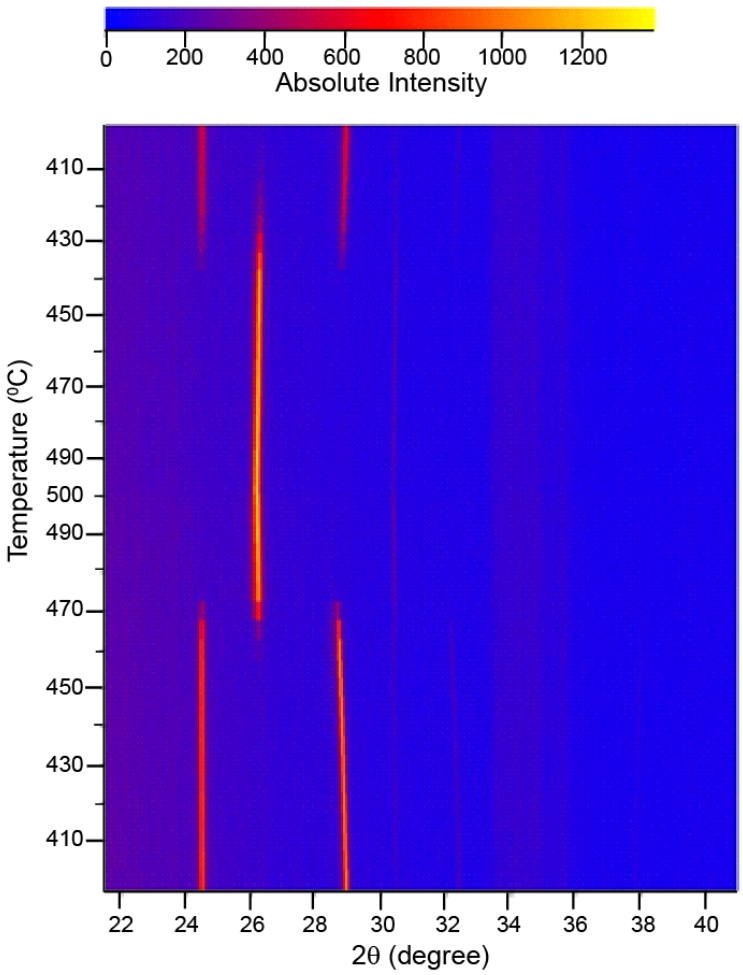

Figure 10. Temperature-dependent course of the Bragg reflections of Li_2C_2 (400°C - 500°C)

Longer diffraction measurement (about 2 h) at room temperature and at 500ºC (figure 11) showed the (almost) pure orthorhombic and cubic phases. (The reflections in the 2θ range between 33º and 36º do not belong to the sample, but are built in by certain settings of the primary beam trap.)

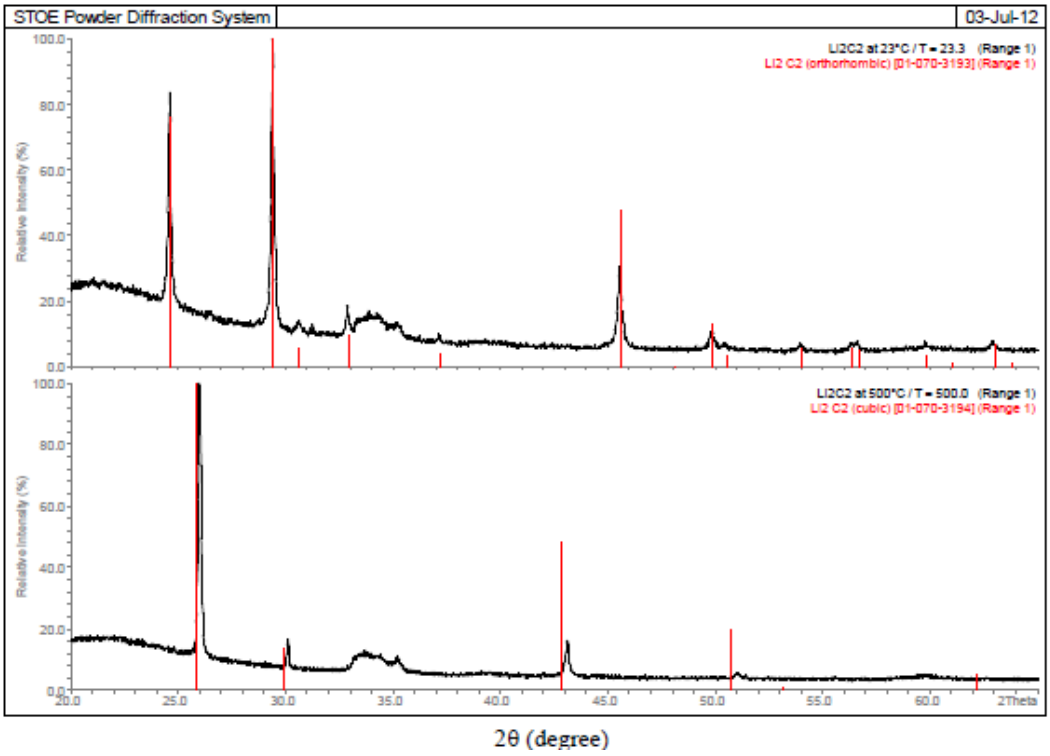

Figure 11. XRD patterns of Li_2C_2 at room temperature and at 500°C (shaded bar graphs with the ICDD PDF database)

A second phase transition was investigated in the range between 700ºC and 850ºC. Unfortunately the sample reacted with quartz and formed Li_2SiO_3 and Li_4SiO_4. It can be concluded from this study that high temperature XRD investigation inside quartz capillary with lithium carbide sample is not applicable for temperatures higher than 600ºC. The probable way out will be neutron measurements inside vanadium containers with $^7Li_2C_2$ sample.

3.2 Room temperature Diamond anvil cell experiments with acetylides

Li_2C_2 and CaC_2, were studied at room temperature by Raman spectroscopy inside a diamond anvil cell to understand the effects of high pressure (up to 30 GPa) on the structural properties of these acetylides.

A complete Raman spectrum was taken at each pressure. Like the ambient pressure condition spectra have been divided into two regions: C-C stretches (between 1800 and 1900 cm^{-1}) and libration modes of C_2 dumbbells and translation modes (between 150 and 500 cm^{-1}).

Pressure dependence of stretching and libration mode of both calcium carbide and lithium carbide were studied by plotting wavenumbers with pressure.

3.2.1 DAC study with CaC_2

A set of Raman spectra of CaC_2 at various pressures has been shown in figure 12 a). With increase of pressure, the intensity of the modes of monoclinic CaC_2-II diminishes and above 2 GPa only CaC_2-I survives (See figure 12 b). Most certainly CaC_2-II either transforms into CaC_2-I at only slightly high pressures, or its Raman spectrum appears to be featureless due to amorphization. It seems that the tetragonal form maintains the spectrum until about 14 GPa where band broadening happens and intensities become weaker. Above 18 GPa, the Raman spectrum of CaC_2 is basically featureless. When the pressure is released, this remains unaffected and thus indicates an irreversible amorphization of CaC_2.

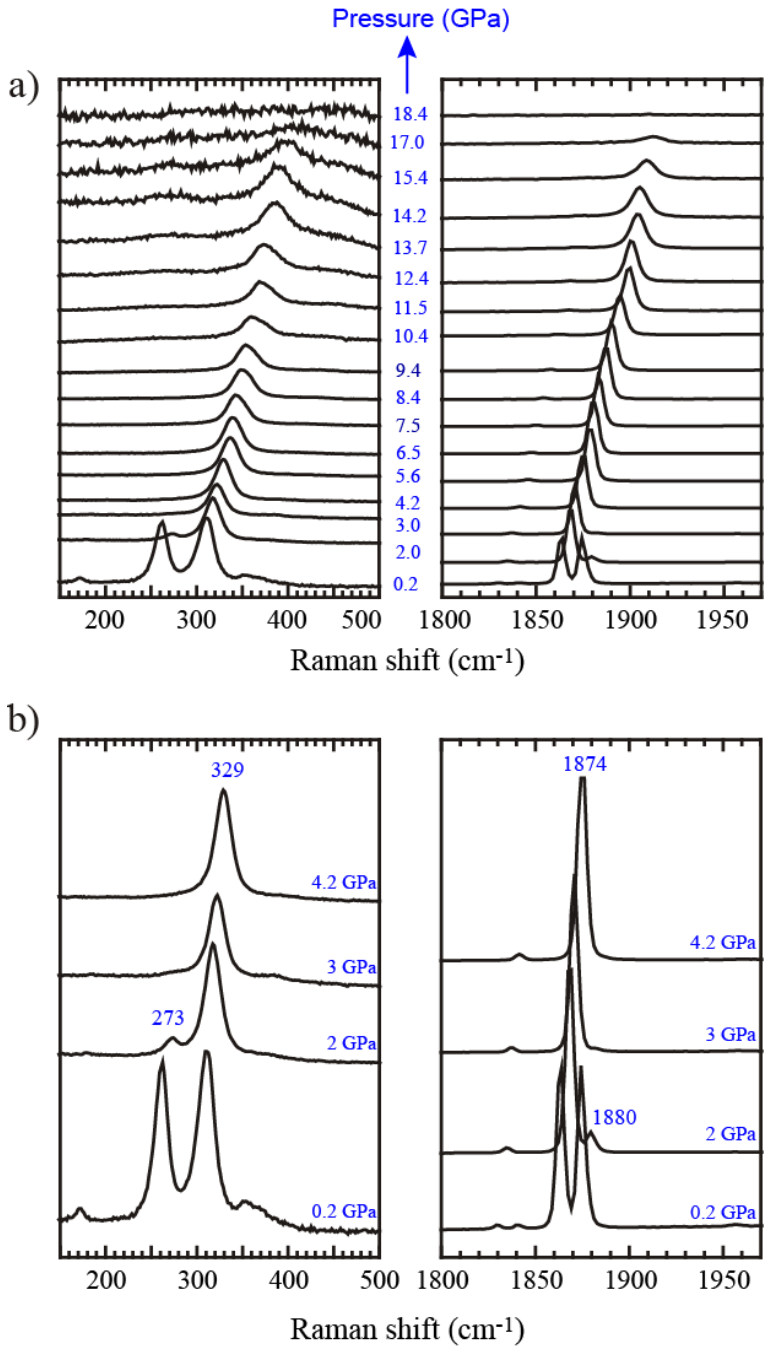

Figure 12. a) Raman spectra of CaC_2 at various pressures. b) Disappearance of CaC_2-II, monoclinic phase at lower pressure region

The pressure dependence of frequencies is plotted in figure 13. A discontinuity may be observed at around 12 GPa, which suggests a distortive

structural transformation of tetragonal CaC_2-I. In conclusion, Raman spectroscopy shows that instability of CaC_2-II with pressure, and indicates a pressure-induced distortion of CaC_2-I followed by the formation of amorphous phase.

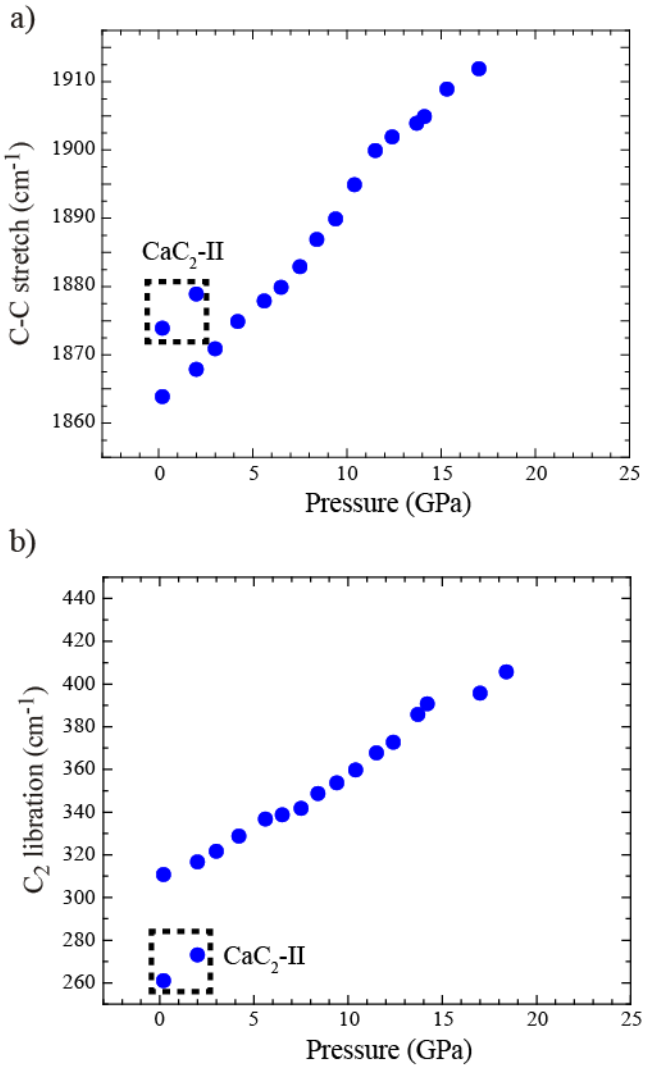

Figure 13: Pressure dependence of stretching and librational modes of CaC_2

3.2.2 DAC study with Li_2C_2

A set of Raman spectra of Li_2C_2 at various pressures has been depicted in figure 14. At around 15 GPa, additional modes appear which is thought

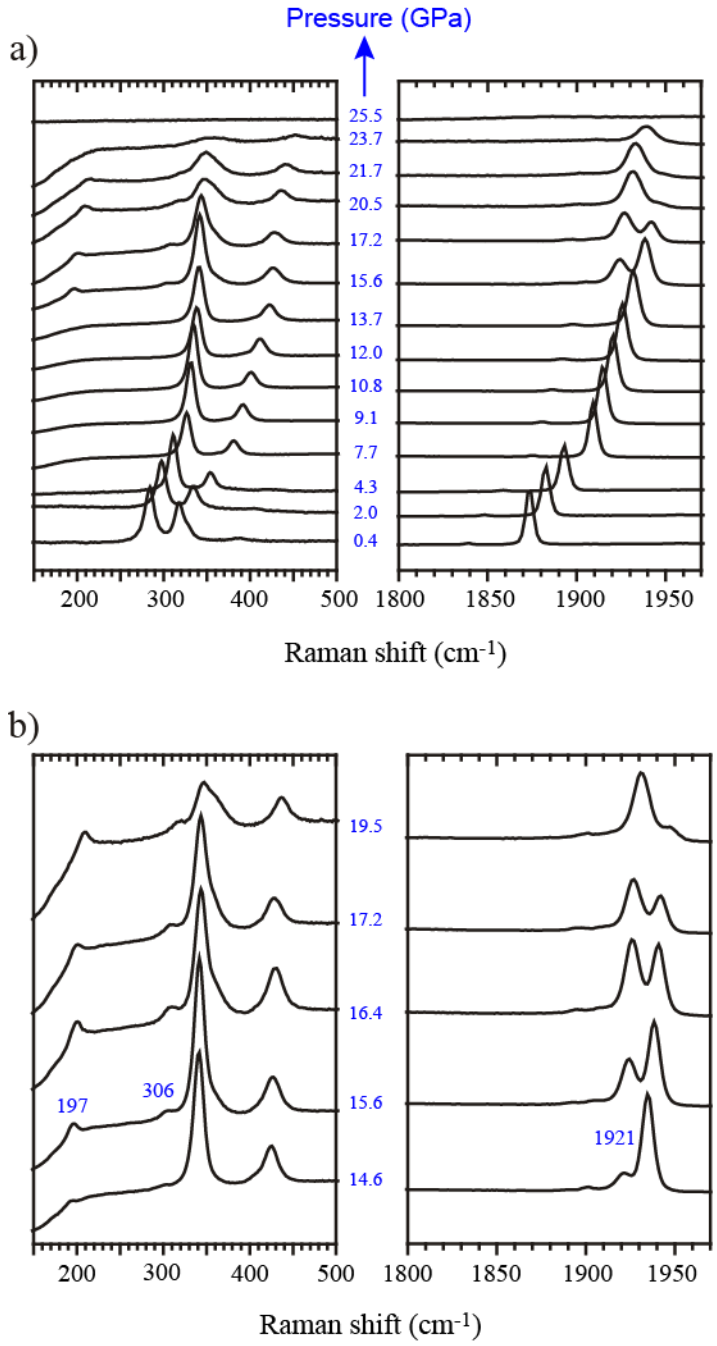

Figure 14: (a) Raman spectra of Li_2C_2 at various pressures. (b) Evolution of high pressure phase

as the beginning of a phase transition. Until about 20 GPa the orthorhombic ground state phase coexists with the high pressure phase. Bands broadening starts above 23 GPa and the Raman spectrum becomes featureless above 25 GPa. This remains unchanged when the pressure is released and an irreversible amorphization of Li_2C_2.is indicated

The development of the high pressure phase and the pressure range of the non-equilibrium two-phase mixture is shown in figure 14b. The occurrence of the high pressure phases is also observed visually as a darkening of the sample in the DAC at about 15 GPa. The C-C stretch of the high pressure phase appears at lower wavenumbers compared to the ground state phase. The more complicated spectrum in the low wavenumber libration-translation region indicates a larger primitive unit cell. The wavenumber of the high frequency mode makes it obvious that the the high pressure phase structure of Li_2C_2 is based on acetylide C_2^{2-} dumbbells and not on zigzag chains of carbon atoms. Thus the observed transition does not match up to the predicted polymerization of dumbbell ions. The subsequent amorphization of Li_2C_2 is observed at higher pressures compared to CaC_2 (25 as against 18 GPa).

Figure 15 depicts the pressure dependence of frequencies. Above 15 GPa, the B_{1g} libration mode of the orthorhombic phase – which has a lower intensity compared to the B_{3g} one – becomes a mode of the high pressure phase, which is indicated by the kink. The structures of alkali metal peroxides and of heavier alkali metal carbides may be considered as possible candidates for the Li_2C_2 high

pressure form. The structure of the high pressure phase is still not conclusive from the study, but may be elucidated from a future X-ray diffraction study.

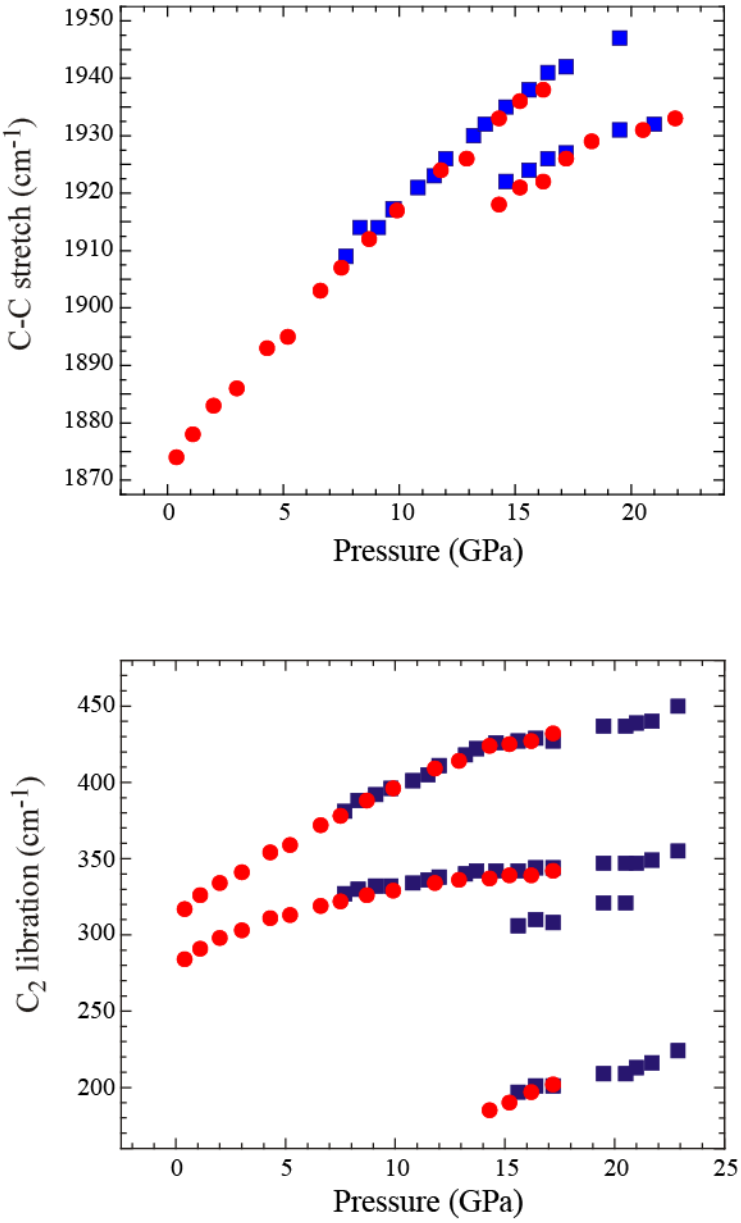

Figure 15: Pressure dependence of stretching and librational modes of Li_2C_2, blue squares and red circles indicate data of different experiments

3.3 High temperature Multi anvil cell experiments with acetylides

3.3.1 Multi anvil cell experiment with CaC_2

A series of multi anvil cell experiments were performed at a constant pressure of 10 GPa and at temperatures of 300ºC, 600ºC and 900ºC.

Table-III MA reaction conditions for CaC_2

Pressure	Temperature	Heating rate	Dwelling time	Capsule
10 GPa	300ºC	5C/min	1 hour	h BN
10 GPa	600ºC	5C/min	1 hour	h BN
10 GPa	900ºC	5C/min	1 hour	h BN
10 GPa	900ºC	5C/min	1 hour	Salt (NaCl)

Products from multi anvil cell experiments were characterized by powder XRD and Raman spectroscopy. Figure 16 and figure 17 depict comparative X-ray diffraction pattern and Raman spectroscopy respectively of multi anvil samples.

300ºC sample: The powder XRD reveals that product is poorly crystalline and most of the CaC_2-II disappears and CaC_2-I survives. In the Raman spectroscopic measurement, peak splitting at C-C stretching is no longer visible, and only one libration mode is present, indicating the presence of one major phase. The wavenumber of C-C stretch drops to 1848 cm^{-1} compared to 1864 cm^{-1} at ambient

pressure and temperature condition. Possible explanation for this lowering of wavenumber may be the less electrostatic interaction of the dumbbell with surrounding cations, as the sample becomes less crystalline after the run. The two humps at 1129 and 1507 cm^{-1} respectively are present which cannot be explained at this moment.

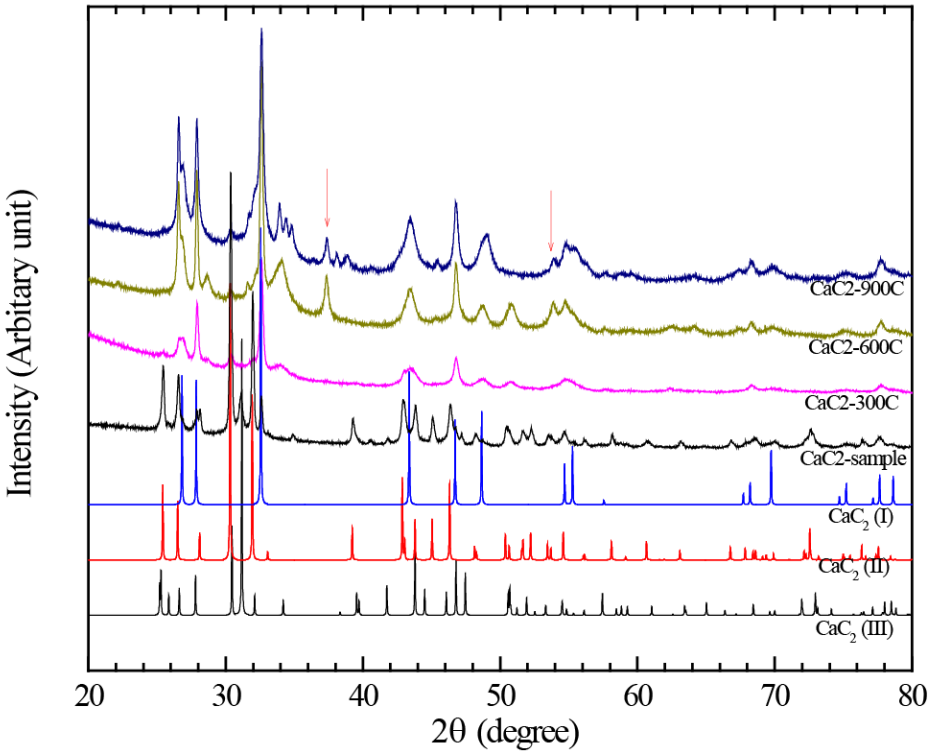

Figure 16. Comparative Powder XRD study: Multi anvil experiments with CaC_2 at fixed pressure (10GPa) and at different temperatures.. Red arrow indicates CaO impurity phase

600ºC sample : Powder XRD reveals sample is more crystalline than 300ºC sample. Peaks corresponding to the CaC_2-I phase are sharper. Sample gets a little oxidized here, and forms CaO and $Ca(OH)_2$. As CaC_2 is highly sensitive to moisture, probably it reacts with moisture during the time it takes to transfer from multi anvil apparatus to glove box after the experiment. A new broad peak starts developing at around two theta equals 34.05 degree, which do not match with any of the CaC_2 known phases. This broad peak may be formed due to overlap of

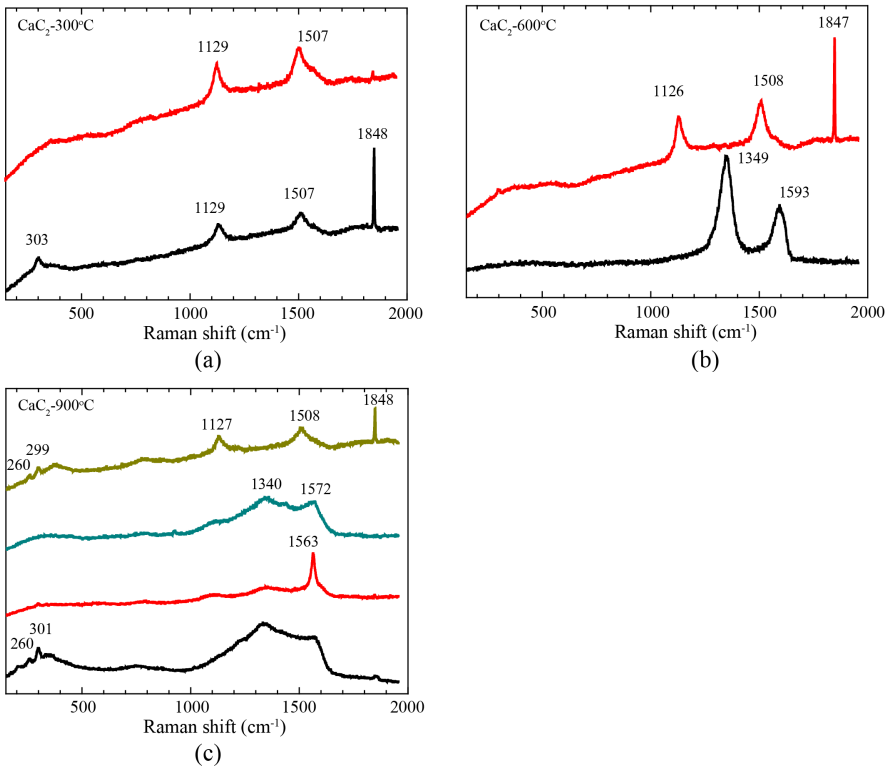

Figure 17. Raman spectra of different parts of CaC_2 multi anvil experiment sample (a) 300ºC (b) 600ºC (c) 900ºC sample

highest intensity peak of $Ca(OH)_2$, and probably some peaks from a new phase. This interpretation will be clear when 900ºC sample will be discussed. Raman spectroscopy shows mostly disordered amorphous carbon feature with a higher intensity D band at around 1349 cm^{-1} and a lower intensity G band at 1593 cm^{-1}. Possible explanation may be some of the CaC_2-II which disappears might turn amorphous at 600°C.

<u>900ºC sample</u> : Sample shows more crystalline nature than 600ºC sample. CaC_2-I is present with a very small amount of CaC_2-II. A tiny amount of CaO impurity is present in the sample but no $Ca(OH)_2$ has been found. The broad peak at two theta equals 34.05 degree of the 600ºC sample splits into three peaks for the 900ºC sample at two theta equal to 33.93, 34.4, 34.82 degrees respectively. The same reaction condition when applied with a different sample container (NaCl capsule), (see figure 18)the powder pattern is reproducible indicating that the new peaks correspond to sole CaC_2 sample and there is no impurity from reaction with capsule material.

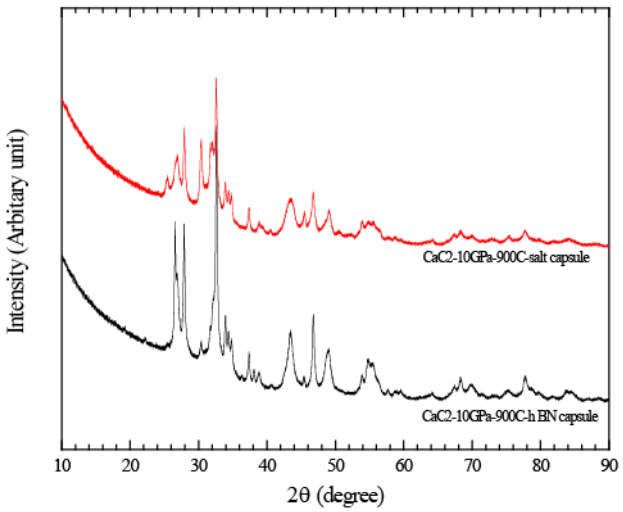

Figure 18. Comparative Powder XRD study: Multi anvil experiments with CaC_2 at fixed pressure (10GPa) and at fixed temperature (900ºC) with different sample capsules (h BN and salt)

Some additional new peaks are also visible in the powder pattern at two theta equal to 31.75 and 32.4 degrees respectively. The Raman measurement does not show any promising new feature. It shows mainly amorphous carbon with D and G band overlap in contrast to the 600ºC sample where D and G band splitting is prominent. Probably the new phase is not Raman active.

These series of runs indicate that higher temperature is needed to obtain a new phase. Hence effort was made to do more runs at higher temperature but the attempt was not successful. The sample environment becomes highly unstable at higher temperature and it is difficult to maintain the temperature for longer time. Another important factor is the choice of capsule materials. Both the NaCl or BN capsule materials have some drawbacks, the former softens rapidly at high

temperatures while the latter can give rise to impurities (e.g. Ca_3BN_3). Therefore investigations into a superior capsule material should be performed.

3.3.2 Multi anvil cell experiment with Li_2C_2

A series of multi anvil cell experiments were performed at a constant pressure of 10 GPa and at temperatures of 300ºC, 600ºC and 900ºC, 1100ºC.

Table-IV: MA reaction conditions for Li_2C_2

Pressure	Temperature	Heating rate	Dwelling time	Capsule
10 GPa	300C	5C/min	1 hour	h BN
10 GPa	600C	5C/min	1 hour	h BN
10 GPa	900C	5C/min	1 hour	h BN
10 GPa	1100C	5C/min	10 mins	h BN
10 GPa	1100C	5C/min	15 mins	NaCl

300ºC sample : : This sample does not show any noticeable change in powder XRD with starting material, other than a less crystalline nature. Raman spectra is also similar to the starting material with an additional peak at around 481 cm^{-1}. Like CaC_2, the wavenumber of C-C stretch appears to be much lower (1852 cm^{-1}) than the one (1872 cm^{-1}) at ambient pressure and temperature condition. Possible explanation may be the less rigidity of dumbbell in Li_2C_2 as the samples become

less crystalline. Here again two humps appear in some spots of the sample at 1121 and 1493 cm^{-1}respectively, which cannot be explained.

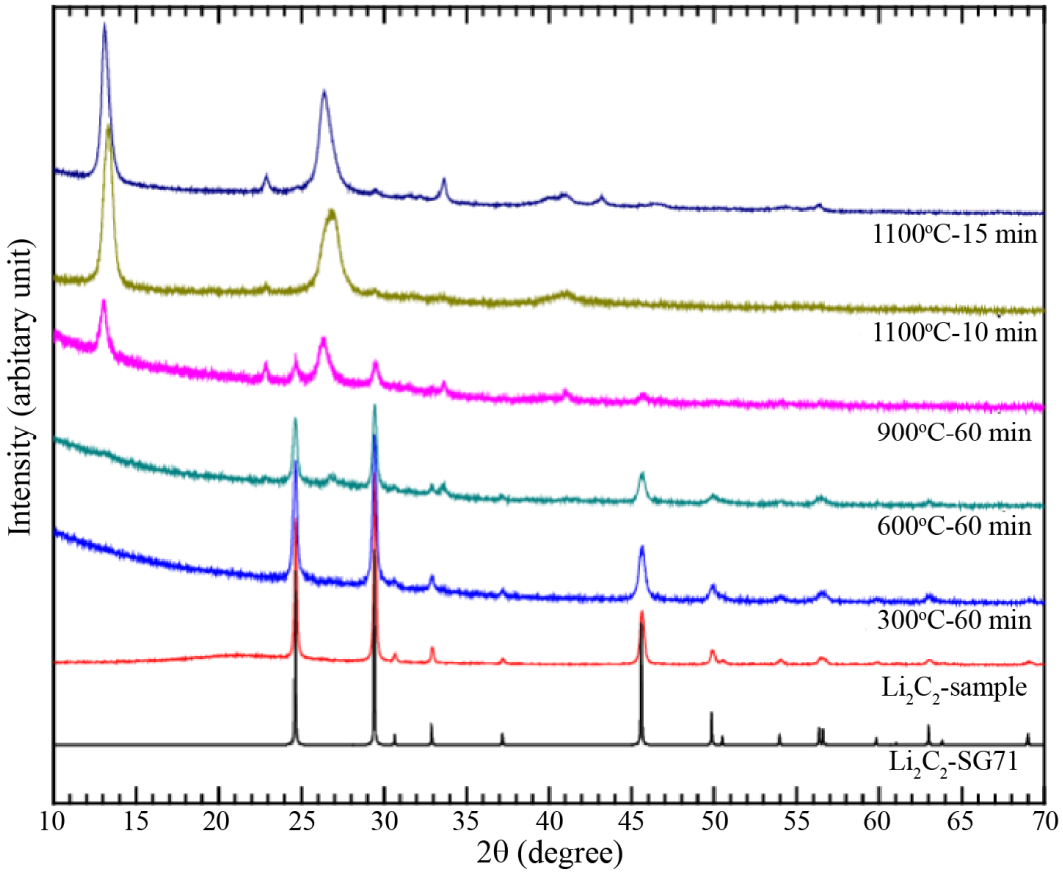

Figure 19. Comparative Powder XRD study: Multi anvil experiments with Li_2C_2 at fixed pressure (10GPa) and at different temperatures

600ºC sample : : The powder XRD reveals some weak reflections in addition to the starting material phase. Raman shows the starting material phase with some amorphous carbon feature. The D and G bands are not well resolved and appear at 1336 and 1552 cm^{-1} respectively. It is quite comparable with the CaC_2 - 900ºC sample.

900ºC sample : The weak additional reflections at 600ºC sample are much prominent for the 900ºC sample. A new phase should be present with the starting material phase. Longer reaction time experiment (4 hours) helped to produce more crystalline new phase but it does not help to get rid of starting material phase (which has not been shown here). Raman spectroscopy of 900ºC sample shows C-C stretching and libration mode comparable with that of starting material. Additionally 900ºC sample shows two sharp humps at 1112 and 1483 cm^{-1} respectively.

1100°C sample : Products at 1100°C were free from starting material. Reactions at 1100°C were very difficult to control and hitherto only short reaction times (about 10 min) could be applied before the sample environment in the pressure cell turned highly unstable. Characteristic of the PXRD patterns for those products are three broad reflections with d spacings of 6.7, 3.4 and 2.3 Å respectively. Additional sharp peaks become visible when a reaction time of 15 min is applied. The Raman spectrum of products at 1100°C display a, most prominent feature, band centered around 1430 cm^{-1} with a shoulder toward lower wavenumbers. It might be guessed that two humps of 900°C sample overlap and form a broad hump here at 1100°C sample. Both the PXRD patterns and Raman spectra of products at 1100°C have not been found in literature for any known carbons or carbides.

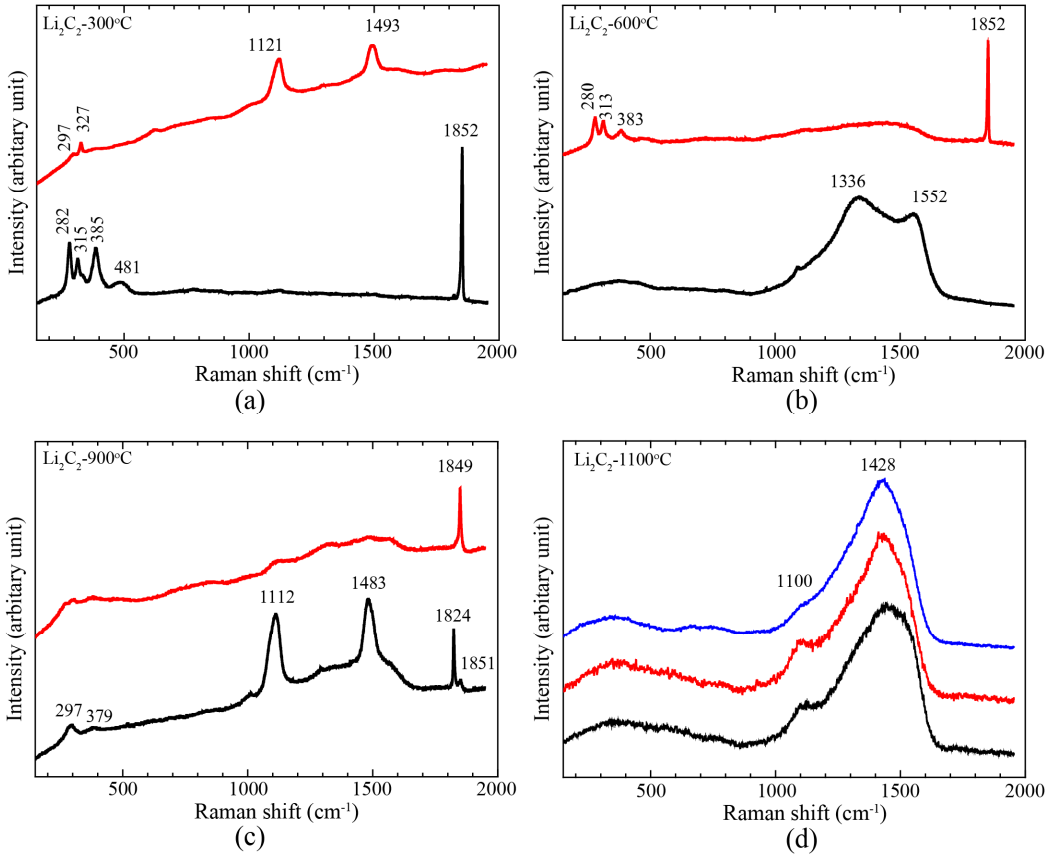

Figure 20. Raman spectra of different parts of Li_2C_2 multi anvil experiment sample (a) 300°C (b) 600°C (c) 900°C and (d) 1100°C sample

Again, these series of runs indicate that higher temperature is needed to obtain a new phase. Therefore investigations into a superior capsule material should be performed.

CHAPTER 4

CONCLUSION

Lithium carbide and calcium carbide have been synthesized and characterized by PXRD and Raman spectroscopy. Thermal behavior of Li_2C_2 has been investigated by DTA experiment in which two phase transitions are observed. The first phase transition from orthorhombic to cubic phase near 420ºC, already reported in literature, is supported by high temperature XRD measurement inside quartz capillary. DTA experimental data on the Li_2C_2 sample indicates the occurrence of a second phase transition around 750ºC to 800ºC. Attempts have been made to explore the details of this transition by high temperature XRD experiment; unfortunately it was unsuccessful as lithium carbide reacts with quartz capillary. One of the possible explanations for this phase transition may be rotational disorder in the acetylide dumbbell.

Inside DAC, Li_2C_2 and CaC_2 have been studied by Raman spectroscopy up to pressures of 30 GPa at room temperature. Li_2C_2 undergoes a transition to a high pressure acetylide phase near 15 GPa. Amorphization of Li_2C_2 is observed around 25 GPa. At ambient pressure CaC_2 contains mainly CaC_2-I and CaC_2-II. Monoclinic CaC_2-II is not stable at pressures above 1 GPa. The Raman spectra of CaC_2 suggest a pressure induced distortion on the CaC_2-I phase after 12 GPa. Analogous to Li_2C_2, finally the CaC_2 also turns amorphous at very high pressure, around 18 GPa. Therefore these pressure induced structural transitions followed by amorphisation is observed for both Li_2C_2 and CaC_2. Similar sequential structural changes are reported for BaC_2.

Multi anvil cell experiments are not conclusive. It has been observed that the sample environment in the MA cell turned extremely unstable of 10GPa pressure when the temperature was higher than 900°C. So short reaction time can be applied at temperatures higher than 900°C. For Li_2C_2, a new phase free of starting material, was found at 1100°C. The PXRD data displays mainly three broad reflections with d-spacings of 6.7, 3.4 and 2.3 Å, respectively. The Raman spectrum of products at 1100°C display a broad band centered around 1430 cm^{-1}, with a shoulder towards lower wavenumbers. Both the PXRD patterns and Raman spectra of products at 1100°C are unique. Longer reaction time may help to form the phase with better crystalline nature. For CaC_2 new additional reflections in PXRD were observed at 900ºC with the starting material phase. To obtain a phase free from starting material, experiments were attempted at higher temperature but were not successful.

Systematic efforts will be required to understand the behavior of Li_2C_2 and CaC_2 at high pressures and high temperatures. This usually includes new experimental conditions such as establishing a stable reaction environment at high temperatures (above 1000°C) and utilizing a proper sample container (for example Ta) for MA experiments. DAC experiments need to be performed at elevated temperatures.

REFERENCES

(1) Aoki, K.; Usuba, S.; Yoshida, M.; Kakudate, Y.; Tanaka, K.; Fujiwara, S. *The Journal of Chemical Physics* **1988**, *89*, 529–534.

(2) Sakashita, M.; Yamawaki, H.; Aoki, K. *The Journal of Physical Chemistry* **1996**, *100*, 9943–9947.

(3) Chad, C.; Badding, J. V. *The Journal of Physical Chemistry A* **2000**, *104*, 8142–8145.

(4) Ceppatelli, M.; Santoro, M.; Bini, R.; Schettino, V. *The Journal of Chemical Physics* **2000**, *113*, 5991.

(5) Bernasconi, M.; Chiarotti, G. L.; Focher, P.; Parrinello, M.; Tosatti, E. *Phys. Rev. Lett.* **1997**, *78*, 2008–2011.

(6) Emery, N.; Hérold, C.; d' Astuto, M.; Garcia, V.; Bellin, C.; Marêché, J. F.; Lagrange, P.; Loupias, G. *Phys. Rev. Lett.* **2005**, *95*, 087003.

(7) Grüneis, A.; Attaccalite, C.; Rubio, A.; Vyalikh, D. V.; Molodtsov, S. L.; Fink, J.; Follath, R.; Eberhardt, W.; Büchner, B.; Pichler, T. *Phys. Rev. B* **2009**, *79*, 205106.

(8) Fleming, R. M.; Rosseinsky, M. J.; Ramirez, A. P.; Murphy, D. W.; Tully, J. C.; Haddon, R. C.; Siegrist, T.; Tycko, R.; Glarum, S. H.; Marsh, P.; Dabbagh, G.; Zahurak, S. M.; Makhija, A. V.; Hampton, C. *Nature* **1991**, *352*, 701–703.

(9) Kulkarni, A.; Doll, K.; Scho□n, J. C.; Jansen, M. *The Journal of Physical Chemistry B* **2010**, *114*, 15573–15581.

(10) Efthimiopoulos, I.; Kunc, K.; Vazhenin, G. V.; Stavrou, E.; Syassen, K.; Hanfland, M.; Liebig, S.; Ruschewitz, U. *Physical Review B* **2012**, *85*.

(11) Wang, X.; Loa, I.; Syassen, K.; Kremer, R. K.; Simon, A.; Hanfland, M.; Ahn, K. *Phys. Rev. B* **2005**, *72*, 064520.

(12) Chen, X.-Q.; Fu, C. L.; Franchini, C. *Journal of Physics: Condensed Matter* **2010**, *22*, 292201.

(13) Juza, R.; Wehle, V.; Schuster, H.-U. *Zeitschrift für anorganische und allgemeine Chemie* **1967**, *352*, 252–257.

(14) Knapp, M.; Ruschewitz, U. *Chemistry-A European Journal* **2001**, *7*, 874–880.

(15) Keppler, H.; Frost, D. J. *EMU notes in mineralogy* **2005**, *7*, 1–30.

(16) Mao, H. K.; Xu, J.; Bell, P. M. *Journal of Geophysical Research* **1986**, *91*, 4673–4676.

(17) Stoyanov, E.; Häussermann, U.; Leinenweber, K. *High Pressure Research* **2010**, *30*, 175–189.

(18) Kroumova, E.; Aroyo, M. I.; Perez-Mato, J. M.; Kirov, A.; Capillas, C.; Ivantchev, S.; Wondratschek, H. *Phase Transitions* **2003**, *76*, 155–170.

(19) Ruschewitz, U.; Pöttgen, R. *Zeitschrift für anorganische und allgemeine Chemie* **1999**, *625*, 1599–1603.